Comparative Study of Mono and Hybrid Nanofluids in MQL Turning of AISI 1040 Steel Using Box–Behnken RSM Approach

Altaf Nalbandh[1,2], Neeraj Chavda[3,4*] and Rakesh Bumataria[2]

[1]Research Scholar, Gujarat Technological University (GTU), Ahmedabad, Gujarat, India
[2]Lecturer, Mechanical Engineering Department, Government Polytechnic, Porbandar, Gujarat, India
[3]Supervisor, Gujarat Technological University (GTU), Ahmedabad, Gujarat, India
[4]Assocaite Professor, Mechanical Engineering Department, G. H. Patel College of Engineering and Technology, The Charutar Vidya Mandal (CVM) University, Vallabh Vidhyanagar, Anand, Gujarat, India

*Corresponding author's email: neeraj_chavda@yahoo.com

DOI: 10.64823/ijter.2604004

Date of Submission: April 12, 2026; Date of Acceptance: April 12, 2026 (Expedited Review); Date of Publication: April 13, 2026

***Abstract*:** The growing emphasis on sustainable manufacturing has increased interest in ecofriendly lubrication strategies for machining. Conventional flood cooling, despite its effectiveness, is associated with high fluid consumption, waste disposal concerns, and occupational health risks, motivating the use of near-dry alternatives such as minimum quantity lubrication (MQL). This study investigates the effect of mono and hybrid nanofluids under MQL on the turning performance of AISI 1040 steel. Three input parameters, cutting speed, feed rate, and nanoparticle weight percentage, were evaluated against three responses, cutting force, cutting temperature, and surface roughness. The experiments were designed using Response Surface Methodology with a Box–Behnken design to develop second order regression models and perform multi-response optimization. The models showed good agreement with the experimental results, confirming their predictive reliability. Among the tested conditions, the hybrid nanofluid Case E (75:25 Al_2O_3:ZnO) provided the best overall performance. The optimal combination of 31.71 m/min cutting speed, 0.11 mm/rev feed, and 1 wt% nanoparticle concentration produced the highest desirability. The findings indicate that mono and hybrid nanofluids under MQL can improve machining performance, with Case E offering the best balance of thermal control and friction reduction. However, the conclusions are limited to the studied parameter range and setup.

***Index Terms*:** Mono Nanofluids, Hybrid Nanofluids, Response Surface Methodology, ANOVA, Al_2O_3, ZnO

I. INTRODUCTION

The increasing demand for cleaner and more efficient manufacturing has encouraged the development of sustainable machining methods that reduce coolant consumption without compromising process performance. In conventional turning operations, cutting fluids are commonly used to reduce heat generation, lower friction, and improve surface quality; however, their extensive use raises concerns related to environmental pollution, operator health, and disposal cost. The flood-cooling constraints could be circumvented by replacing the cutting fluid with wet machining, as in dry machining [1]. For this reason, A novel, economical, and practical approach to MQL has emerged as a promising near-dry machining approach for reducing fluid usage while maintaining acceptable cooling and lubrication at the cutting zone [2]. The alternative strategy of mist lubrication, where an air-cutting fluid mixture is supplied to the cutting zone and is more readily accessible due to the high pressure, has proven to be a superior option for coolant system applications [3]. The nozzle was used to mix the

lubricant/coolant with oil, producing an aerosol. To achieve better cooling, spray the aerosol into the cutting zone at high pressure [4]. MQL is an effective alternative that minimizes fluid usage by delivering a small, targeted amount of lubricant directly to the cutting interface without compromising lubrication quality.

A comparative evaluation between MQL and wet machining of AISI 1045 steel was conducted, using fractional factorial design via MINITAB was employed for factor screening, followed by a Central Composite Design (CCD) under the RSM framework for process optimization. While the resulting cutting force models demonstrated high predictive accuracy, the surface roughness models exhibited lower correlation during validation [5]. Leppert [6] evaluated dry, MQL, and emulsion cooling during turning of AISI 1045 steel, noting higher cutting forces without adequate fluid, especially at low feed rates. Che Haron et al. [7] employed RSM to investigate the impact of turning parameters on the surface integrity of Inconel 718. The study evaluated multiple performance characteristics, including surface roughness, microstructure, topography, and microhardness, ultimately identifying feed rate as the most significant factor influencing surface roughness. Hadad & Sadeghi [8] investigated MQL nozzle position and parameters in turning AISI 4140 steel, finding it significantly lowered temperatures and forces; they validated a heat source/sink temperature model experimentally. Liu et al.[9] utilized RSM to investigate the effects of flexible coupling under MQL conditions. The study identified feed rate as the primary driver for both surface roughness and cutting force, concluding that these responses are minimized when employing a combination of low feed rate, shallow depth of cut, and high cutting speed. Saini et al. [10] investigated the impact of turning parameters on cutting forces and tool-tip temperatures during the machining of AISI 4340 steel. The study compared the performance of PVD and CVD-coated inserts, concluding that PVD-coated tools exhibited superior performance compared to their CVD counterparts. Agrawal & Patil [11] tested aloe vera oil versus conventional Servo cut S oil on M2 steel, achieving 6.7% lower surface roughness and 0.14% less tool wear with the bio-lubricant. Sivaiah et al. [12] conducted a comparative study on the machining of AISI 52100 steel using MQL in conjunction with textured and untextured cutting tools. The findings revealed that the integration of textured tools significantly enhanced machining performance, yielding a 42% reduction in surface roughness, a 40% decrease in flank wear, and a 25% reduction in cutting temperatures compared to untextured variants. Singh et al. [13] employed Response Surface Methodology (RSM) based on a Central Composite Design (CCD) to optimize the turning of Hastelloy C-276 under vegetable oil-based MQL. The study successfully identified an optimal parameter set that simultaneously minimized cutting temperature and surface roughness while maximizing the chip reduction coefficient. Sivaiah et al. [14] investigated the efficacy of MQL-assisted turning of AISI 304 steel using tungsten carbide tools featuring circular micro-pit textures. The experimental results demonstrated significant performance gains, including a 54% reduction in surface roughness, a 7% decrease in tool wear, and a 27% increase in the material removal rate compared to conventional tooling.

Nanofluids have further expanded the capability of MQL by enhancing the thermal and tribological properties of the base fluid through the addition of nanoparticles. Nanofluids, formed by dispersing solid nanoparticles in a base fluid, can significantly enhance the thermal and tribological performance of MQL systems by improving heat transfer and reducing friction at the tool–chip interface. Hybrid nanofluids, such as Al_2O_3–ZnO suspensions, combine different nanoparticles to exploit synergistic effects, offering higher thermal conductivity, better stability, and improved anti-wear and anti-friction behaviour compared with mono-nanofluids [15], [16], [17], [18]. These characteristics can translate into lower cutting temperatures, reduced cutting forces, and improved surface quality in metal cutting processes. However, the combined influence of process parameters and nanoparticle concentration on multi-response machinability in turning AISI 1040 under MQL remains insufficiently quantified. The Box-Behnken design within the Response Surface Methodology (RSM) framework is an economical alternative for modeling machining processes. It provides a strategic balance between experimental cost and data accuracy, allowing for the derivation of precise empirical relationships between process variables and multiple output responses.

Padmini et al.[19] conducted an experimental investigation into the turning of AISI 1040 steel using nano-boric acid (50 nm) suspensions in SAE-40 and coconut base oils. The nanofluids were prepared at various weight concentrations and subjected to ultrasonic processing for one hour to ensure uniform dispersion. The study

evaluated the effects of these lubricants on critical machining outputs, including cutting temperature, surface roughness, and tool flank wear. [20] investigated the influence of Carbon Nanotube (CNT) based nanofluids on the turning performance of AISI 1040 steel. The study focused on critical machining outputs, including tool-workpiece interface pressures, cutting temperatures, surface integrity, and tool wear. Experimental results indicated that these parameters were significantly enhanced with CNT concentrations up to 2 wt%. Amrita et al. [21] investigated the performance of nanographite (80 nm) enhanced mist lubrication during the turning of AISI 1040 steel with cemented carbide and High-Speed Steel (HSS) tools. The study compared this nano-mist environment against conventional dry, flood, and graphite-free mist conditions. Experimental results revealed a significant reduction in both tool wear and cutting forces for both tool materials compared to traditional dry and flood lubrication.

The impact of Graphite (80 nm), boric acid (100 nm), and MoS2 (100 nm) nanosuspensions in emulsifier oil under MQL conditions was evaluated by [22]. The turning experiments on AISI 1040 steel highlighted the different lubrication and cooling capabilities of these three nanoparticle types with stability of nanofluids containing 0.3 wt % nanoparticles and these cutting fluids were flowed at 10 ml/min. Sharma et al. [4], [23] checked the efficacy of MQL-assisted turning of AISI 1040 steel using TiO_2 and Al_2O_3 nanofluids dispersed in a vegetable oil-water emulsion. Compared to dry, mist, and wet machining environments, the nanofluid application significantly reduced surface roughness and tool wear. Furthermore, an improvement in chip morphology was observed, characterized by the formation of silver-colored, curled, and segmented chips, indicating efficient heat dissipation at the cutting zone. Rapeti et al. [24] investigated the performance of vegetable-based nano-cutting fluids, including coconut, canola, and sesame oils, enriched with Molybdenum disulfide (MoS_2) nanoparticles for the turning of AISI 1040 steel. To achieve multi-objective optimization, Taguchi-based Grey Relational Analysis (GRA) was employed. The findings indicated that coconut oil containing 0.5 wt% nano-MoS_2 yielded superior machining performance at an optimal cutting speed of 40 m/min and a feed rate of 0.14 mm/rev. Pasam et al. [25] conducted an experimental study on the development and testing of vegetable oil-based nano and micro-fluids for the MQL assisted turning of AISI 1040 steel. Both boric acid (100 nm) and MoS_2 (90 nm) were dispersed in coconut oil as the base fluid. The results indicated that nanofluids exhibited superior performance compared to their micro-scale counterparts at high cutting speeds, whereas both demonstrated comparable efficacy at lower speed regimes. Padmini et al. [26] focused on the performance of Molybdenum disulfide (MoS_2) based nanofluids, utilizing various vegetable oils (coconut, sesame, and canola) as base fluids for the MQL-assisted machining of AISI 1040 steel. The study revealed that the addition of 0.5 wt% MoS_2 to coconut oil led to a significant reduction in cutting temperatures, tool wear, cutting forces, and surface roughness. These results confirmed the superior efficacy of this specific nano-lubricant formulation over alternative lubrication strategies. Sharma et al. [3] investigated the impact of various SiO_2 nanoparticle concentrations dispersed in a vegetable oil-water emulsion during the turning of AISI 1040 steel. The study compared dry machining and MQL-assisted nanofluid application against conventional cooling methods through a series of experiments. The results demonstrated that the integration of SiO_2 nanofluids with MQL significantly reduced cutting forces compared to both dry machining and traditional flood cooling operations.

Sharma et al. [27] conducted an experimental analysis of the turning of AISI 304 steel using a hybrid nanofluid composed of Al_2O_3 (45 nm) and MoS_2 (30 nm) in a 9:1 ratio. The hybrid nanoparticles were dispersed at volume concentrations of 0.25%, 0.75%, and 1.25 v%. The results demonstrated a significant reduction in machining responses, specifically achieving maximum decreases of 18.08% in Fx, 5.73% in Fy, 7.35% in Fz, and 2.38% in surface roughness. Singh et al. [28] conducted numerical simulations to evaluate the impact of incorporating graphene nanoplatelets into an Al-based nanofluid at volume concentrations of 0.25%, 0.75%, and 1.25 v%. The study demonstrated that increasing the nanoparticle concentration led to a significant enhancement in thermal conductivity and viscosity, while simultaneously improving the wear resistance of the hybrid nanofluid. Sharma et al. [27] investigated the performance of hybrid nanofluids composed of Al_2O_3 and Graphene Nanoplatelets (GnP) during the turning of AISI 304 steel. The hybrid suspensions were developed at volume concentrations of 0.25%, 0.75%, and 1.25 vol.%. Tribological and wettability characterization revealed that the hybrid formulations exhibited the lowest friction coefficients and pin wear. Furthermore, machining results

demonstrated a 5.29% reduction in cutting temperature and a 12.29% decrease in tool wear compared to conventional Al_2O_3 based nanofluids. Jamil et al. [29] studied the usefulness of cryogenic cooling (CO_2) and MQL in turning tungsten alloys. Al_2O_3 (30 nm) and MWCNT (10-30 nm) are suspended in a vegetable oil-based fluid for nanofluid preparation. Taguchi's L9 orthogonal array was used for experiments design using with cutting Speed, feed rate, and cooling techniques as design variables. It was seen from the results that the mean surface roughness was retard by 8.72%, the machining cutting force by 11.8%, and the tool life was enhanced by 23% with hybrid nanofluids in contrast to CO_2 cooling. Yıldırım [30] experimentally investigated the impact of various cooling strategies including dry, MQL, cryogenic, and nanofluid-based approaches—on the turning of Inconel 625. The study utilized a hybrid nanofluid composed of Al_2O_3 (70 nm) and hBN (70 nm) at different concentration ratios, while LN2 was employed for cryogenic cooling. By evaluating surface roughness, tool wear, and tool-chip interface temperatures, the results indicated that a 0.5 v% hBN concentration optimized the machining responses, particularly in reducing thermal loads and surface friction.

Thakur et al. [31] experimentally evaluated the impact of various cooling strategies including MQL, mono nanofluid + MQL, and hybrid nanofluid + MQL on the turning of EN 24 steel. Water-based lubricants were enriched with Al_2O_3, CuO, and Al_2O_3-CuO nanoparticles at concentrations of 0.5%, 1%, and 1.5 wt%. Following a comparative investigation, the results demonstrated that the hybrid (Al_2O_3-CuO) nanofluids exhibited superior machining performance compared to their mono-nanofluid counterparts. Zaman et al. [32] investigated the influence of machining parameters—specifically cutting speed, feed rate, depth of cut, nanoparticle concentration, and tool type on the turning of Ti-6Al-4V alloy under hybrid Al_2O_3-MWCNT nanofluid-based MQL. Utilizing a Box-Behnken experimental design and RSM, empirical models were developed for cutting temperature and surface roughness. The results indicated that cutting temperature increased with higher speeds, feeds, and depths of cut. Interestingly, as nanoparticle concentration increased, the temperature initially reached a minimum threshold before rising again. Additionally, feed rate was identified as the most significant factor affecting surface roughness. Sandeep Kumar et al. [33] examined the performance of hybrid Cu-Zn nanofluids using groundnut oil as a base fluid during the MQL-assisted turning of Inconel 718. The experiments were conducted using Ti-coated carbide inserts under three distinct environments: dry cutting, MQL with pure vegetable oil, and MQL with the hybrid nanofluid. The investigation revealed that the hybrid nanofluid MQL approach achieved a significant reduction in both cutting temperature and surface roughness compared to both dry and conventional vegetable oil-based MQL conditions.

Sandeep Kumar et al. [34] examined performance of a 50:50 hybrid CuO-ZnO nanofluid using palm and coconut oils as base fluids during the machining of AISI 1018 steel. The study compared the efficacy of these hybrid nano-lubricants against a dry machining environment. The results demonstrated a significant reduction in surface roughness, with statistical analysis identifying feed rate as the most influential parameter, followed by cutting speed and depth of cut. Haghnazari & Abedini [35] processed the machining of AISI 4340 steel using an MQL-based hybrid nanofluid consisting of Al_2O_3 and CuO. The study analyzed the effects of cutting speed, feed rate, and CuO weight percentages (ranging from 0% to 1%) on cutting forces and surface roughness. The experimental results indicated that a hybrid composition of 75:25 (Al_2O_3:CuO) yielded the minimum cutting force at low feed rates and high cutting speeds, while the lowest surface roughness was achieved at low feed rates and moderate cutting speeds.

Despite extensive research on nanofluid-assisted machining, most studies focus on either mono nanofluids or hybrid nanofluids in isolation, often applied to different work materials or without multi-response statistical optimization in a unified framework. In particular, the comparative performance of mono and hybrid nanofluids under MQL during turning of AISI 1040 steel, considering cutting force, cutting temperature, and surface roughness, has not been systematically quantified using RSM with Box–Behnken design. The present work addresses this gap by developing separate three-factor, three-response quadratic models for both mono and hybrid nanofluid cases and by identifying nanofluid-specific optimal operating conditions in terms of cutting speed, feed, and nanoparticle weight percentage. This study therefore offers new insights into the selection and tuning of mono versus hybrid metal-oxide nanofluids for sustainable MQL-assisted turning of AISI 1040 steel.

II. OBJECTIVES

The present study aims to compare the machining performance of two mono nanofluid cases and three hybrid nanofluid cases under MQL during turning of AISI 1040 steel. The work focuses on evaluating how different nanofluid formulations influence cutting force, cutting temperature, and surface roughness under the same machining framework, since nanofluids are widely reported to improve cutting performance and surface integrity in MQL-assisted machining.

The specific objectives are to investigate the effects of cutting speed, feed rate, and nanoparticle weight percentage on the selected responses; to develop statistically valid predictive models using Response Surface Methodology (RSM) with Box–Behnken design; and to identify the significant main and interaction effects for each nanofluid case. Another objective is to determine the best-performing mono and hybrid nanofluid among the selected cases and to establish the optimal machining conditions for that case, so that the comparative performance can be interpreted in terms of both thermal and mechanical behaviour. Finally, the study seeks to assess whether hybrid nanofluids provide a measurable advantage over mono nanofluids in sustainable machining and to support practical parameter selection for improved turning performance of AISI 1040 steel.

III. MATERIALS & METHODS

In the present study, the experimental design was formulated using Response Surface Methodology (RSM) to analyze the influence of process variables on the machining outputs. This structured Design of Experiments (DOE) approach enhances the efficiency of the investigation by minimizing experimental time and costs. Three primary input parameters were investigated: cutting speed (31.71, 69.63, and 107.55 m/min), feed rate (0.11, 0.18, and 0.25 mm/rev), and nanoparticle concentration (0%, 1%, and 2 wt%). The specific factor levels are summarized in Table 1.

Table 1. Level for input parameters for RSM Box Behnken Method

Input parameters	Low (-1)	High (1)	Center (0)
Cutting Speed (m/min)	31.71	107.55	69.63
Feed (mm/rev)	0.11	0.25	0.18
Wt % of nanoparticle (%)	0	2	1

The nanofluids used in this study were formulated using the two-step method. For the mono-nanofluids, Aluminium Oxide (Al_2O_3) and Zinc Oxide (ZnO) nanoparticles of identical size were dispersed into 100 ml of SAE-40 base oil. The hybrid nanofluids were prepared by blending the two nanoparticle types in a predetermined ratio before dispersion. To ensure uniform particle distribution and long-term stability, each mixture underwent 2 hours of magnetic stirring followed by 2 hours of ultrasonication. The technical specifications for all nanoparticles are summarized in Table 2.

The nanoparticle size was restricted to the 30–50 nm range to maximize thermal conductivity enhancement while minimizing the risk of agglomeration. This range ensures optimal dispersion and sprayability within the MQL system [36]. Furthermore, the weight concentration was set between 0-2 wt.% based on a review of existing machining literature. Studies indicate that concentrations below 0.5 wt.% offer marginal performance gains, whereas concentrations exceeding 1.5-2 wt.% tend to increase fluid viscosity. Such high loadings can lead to nozzle clogging and poor atomization, ultimately degrading the surface finish and increasing cutting forces [37], [38].

Table 2. Technical specifications of nano particles

Technical Specifications	Aluminium Oxide	Zinc Oxide
Molecular Formula	Al_2O_3	ZnO

Purity (%)	99.90	99.90
Average particle size (nm)	30-50	30-50
True Density (g/cm^3)	3.97	4.97
Bulk Density (g/cm^3)	1.5	-
Specific Surface area (m^2/g)	120-140	90-110
Molecular Weight (g/mol)	101.96	81.408
Morphology	Spherical	Spherical
Colour	White	Milky White
Physical form	Powder	Powder

The nanofluids were delivered via a specialized MQL system comprising a fluid reservoir, a precision pressure valve, a mixing chamber, and a 2 mm diameter nozzle. To ensure consistent lubrication and cooling, a constant air pressure of 3 bar and a lubricant flow rate of 360 mL/hr were maintained throughout the experiments. The workpieces utilized were AISI 1040 steel rods, each measuring Ø50×300 mm.

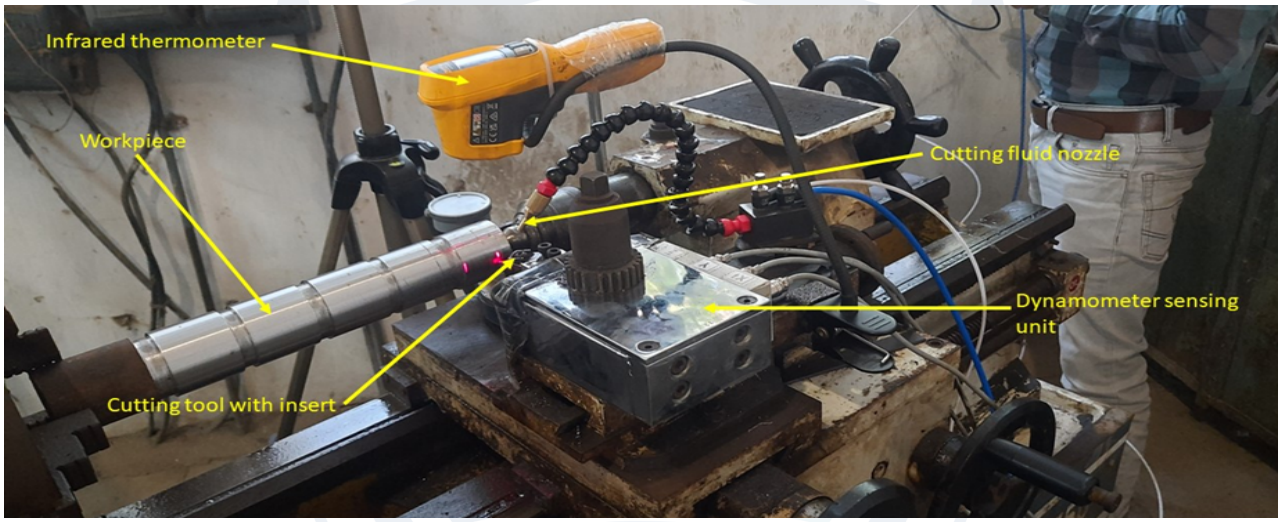

Fig. 1 Experimental set up

The turning experiments were conducted on a Banka 35-750 geared lathe (Banka Machine Pvt. Ltd.) utilizing a Deskar TNMG160408 CQ LF9218 cutting tool. A strain gauge-based, bridge-form lathe tool dynamometer was employed to monitor the cutting forces. To characterize the thermal and surface properties, a Fluke 62 Max+ digital infrared thermometer was used for measuring the cutting temperature, while a Mitutoyo SJ-210 portable tester was used to evaluate the surface roughness of the workpiece. Throughout the experimental runs, the depth of cut was maintained at a constant value of 0.6 mm. The complete experimental configuration is illustrated in Fig. 1, and the comprehensive testing parameters are detailed in Table 3.

Table 3. Details of experimentation and cutting conditions

Workpiece	
Material	AISI 1040 steel
Size	50 mm (Diameter) × 300 mm (Length)
Cutting fluid	
Cutting fluid	SAE-40 Oil
Nanoparticle	
Aluminium Oxide (Al_2O_3)	30-50 nm
Zinc Oxide (ZnO)	30-50 nm
Weight percentage of nanoparticles	0%, 1%, 2%

Input machining parameters	
Cutting speed	31.71, 69.63, 107.55 m/min
Feed rate	0.11, 0.18, 0.25 mm/rev
Depth of cut	0.6 mm
MQL	
Nozzle diameter	2 mm
Nano fluid discharge	360 mL/hr
Air Pressure	3 bar
Machine tools and measuring devices	
Lathe	Banka 35 750 geared type
Cutting tool (insert)	Deskar TNMG160408 CQ LF9218
Cutting force	Dynamometer strain gauge based bridged form type
Cutting temperature	Fluke 62 Max+ digital infrared thermometer
Surface Roughness	Mitutoyo SJ-210 portable tester

The Response Surface Methodology (RSM) was implemented using a Box-Behnken Design (BBD) to evaluate the interactions between the machining parameters. For each cooling environment, 17 experimental runs were meticulously designed to capture the quadratic effects of the input factors. The various cooling and lubrication strategies investigated in this study are categorized and detailed in Table 4.

Table 4. Cooling strategies with type of NF

Cooling strategy	Type of NF with MQL
Case A	Mono (Al_2O_3)
Case B	Mono (ZnO)
Case C	Hybrid [Al_2O_3:ZnO (25:75)]
Case D	Hybrid [Al_2O_3:ZnO (50:50)]
Case E	Hybrid [Al_2O_3:ZnO (75:25)]

IV. RESULTS

A comprehensive experimental campaign consisting of 85 trials was conducted on AISI 1040 steel to evaluate five distinct cooling strategies (Cases A to Case E). For each experimental run, the cutting force, cutting temperature, and surface roughness were systematically recorded. The complete Response Surface Methodology (RSM) design matrices, including all input parameters and measured output responses for Cases A, B, C, D, and E, are presented in Table 5, Table 6, Table 7, Table 8 and Table 9 respectively.

Table 5. RSM tests with input and output values for Case A

Test Run	Input parameters			Output parameters		
	A:Cutting Speed	B:Wt% of Al_2O_3 NP	C:Feed	Cutting Force	Cutting Temperature	Surface Roughness
	m/min	%	mm/rev	N	°C	µm
1	107.55	0	0.18	340.02	97.84	3.599
2	31.71	0	0.18	320.39	66.17	3.563
3	69.63	1	0.18	209.18	66.5	3.806
4	31.71	2	0.18	280.20	71.83	3.439
5	31.71	1	0.25	137.30	66.33	5.211
6	69.63	1	0.18	201.04	66	4.057

7	69.63	1	0.18	232.62	67.94	4.382
8	69.63	1	0.18	230.07	73.15	3.867
9	69.63	2	0.11	235.37	77.5	2.498
10	31.71	1	0.11	129.16	52.67	2.759
11	69.63	0	0.25	392.28	93.33	4.54
12	69.63	2	0.25	407.78	84.83	3.086
13	69.63	1	0.18	217.42	63.5	4.123
14	69.63	0	0.11	317.84	80.82	3.318
15	107.55	1	0.11	150.34	55	3.494
16	107.55	1	0.25	369.43	89.33	2.252
17	107.55	2	0.18	361.98	84.83	2.334

Table 6. RSM tests with input and output values for Case B

Test Run	Input parameters			Output parameters		
	A:Cutting Speed	B:Wt% of ZnO NP	C:Feed	Cutting Force	Cutting Temperature	Surface Roughness
	m/min	%	mm/rev	N	°C	µm
1	107.55	0	0.18	304.02	97.84	3.599
2	31.71	0	0.18	320.39	72	4.563
3	69.63	1	0.18	348.15	74	2.506
4	31.71	2	0.18	143.87	50.33	3.937
5	31.71	1	0.25	408.66	80	3.911
6	69.63	1	0.18	357.96	73	2.567
7	69.63	1	0.18	377.57	79.56	2.823
8	69.63	1	0.18	382.67	81.4	2.757
9	69.63	2	0.11	101.31	52.33	3.843
10	31.71	1	0.11	215.75	47	2.459
11	69.63	0	0.25	392.28	93.33	4.54
12	69.63	2	0.25	245.18	61.67	4.177
13	69.63	1	0.18	392.28	81	3.082
14	69.63	0	0.11	317.84	80.82	3.318
15	107.55	1	0.11	192.90	70	2.194
16	107.55	1	0.25	393.95	65	3.082
17	107.55	2	0.18	147.10	70	2.769

Table 7. RSM tests with input and output values for Case C

Test Run	Input parameters			Output parameters		
	A:Cutting Speed	B:Wt% of NP	C:Feed	Cutting Force	Cutting Temperature	Surface Roughness
	m/min	%	mm/rev	N	°C	µm
1	107.55	0	0.18	303.99	97.84	3.599
2	31.71	0	0.18	320.36	66.17	3.563
3	69.63	1	0.18	214.06	68.33	3.864
4	31.71	2	0.18	207.59	50.5	4.49

5	31.71	1	0.25	253.29	59	4.64
6	69.63	1	0.18	223.58	68.53	3.892
7	69.63	1	0.18	218.38	69.33	3.86
8	69.63	1	0.18	251.13	76.26	4.246
9	69.63	2	0.11	135.72	49.08	3.584
10	31.71	1	0.11	147.09	51	2.67
11	69.63	0	0.25	392.24	93.33	4.54
12	69.63	2	0.25	282.71	46	5.026
13	69.63	1	0.18	239.76	75.16	4.182
14	69.63	0	0.11	317.81	80.82	3.318
15	107.55	1	0.11	147.09	69.67	2.621
16	107.55	1	0.25	243.48	75.67	4.688
17	107.55	2	0.18	241.82	58.83	4.312

Table 8. RSM tests with input and output values for Case D

Test Run	Input parameters			Output parameters		
	A:Cutting Speed	B:Wt% of NP	C:Feed	Cutting Force	Cutting Temperature	Surface Roughness
	m/min	%	mm/rev	N	°C	µm
1	107.55	0	0.18	303.99	97.84	3.599
2	31.71	0	0.18	338.31	72	4.269
3	69.63	1	0.18	237.01	58	4.242
4	31.71	2	0.18	231.23	53.61	4.297
5	31.71	1	0.25	287.61	50.17	4.559
6	69.63	1	0.18	245.15	60.33	3.958
7	69.63	1	0.18	235.34	60.27	4.16
8	69.63	1	0.18	260.74	65	4.339
9	69.63	2	0.11	145.42	49.08	3.78
10	31.71	1	0.11	166.70	46.83	3.974
11	69.63	0	0.25	392.24	93.33	4.54
12	69.63	2	0.25	265.94	62.22	4.68
13	69.63	1	0.18	250.05	59.8	4.142
14	69.63	0	0.11	295.16	80.82	3.489
15	107.55	1	0.11	166.70	58.87	3.539
16	107.55	1	0.25	253.29	63.33	4.07
17	107.55	2	0.18	233.28	70.88	4.068

Table 9. RSM tests with input and output values for Case E

Test Run	Input parameters			Output parameters		
	A:Cutting Speed	B:Wt% of Al_2O_3 NP	C:Feed	Cutting Force	Cutting Temperature	Surface Roughness
	m/min	%	mm/rev	N	°C	µm
1	107.55	0	0.18	303.99	97.84	3.719
2	31.71	0	0.18	337.23	69.55	3.69

3	69.63	1	0.18	233.68	55.27	4.159
4	31.71	2	0.18	294.18	55.55	4.143
5	31.71	1	0.25	346.45	53.03	4.712
6	69.63	1	0.18	243.48	56.54	4.159
7	69.63	1	0.18	250.05	56.73	4.223
8	69.63	1	0.18	257.02	60.8	4.375
9	69.63	2	0.11	150.33	54.06	3.701
10	31.71	1	0.11	148.76	43.21	2.996
11	69.63	0	0.25	392.24	93.33	4.54
12	69.63	2	0.25	346.84	62.72	4.979
13	69.63	1	0.18	245.15	58	4.267
14	69.63	0	0.11	297.81	80.82	3.318
15	107.55	1	0.11	156.90	56.47	3.867
16	107.55	1	0.25	269.67	64.49	4.546
17	107.55	2	0.18	259.27	63.75	4.845

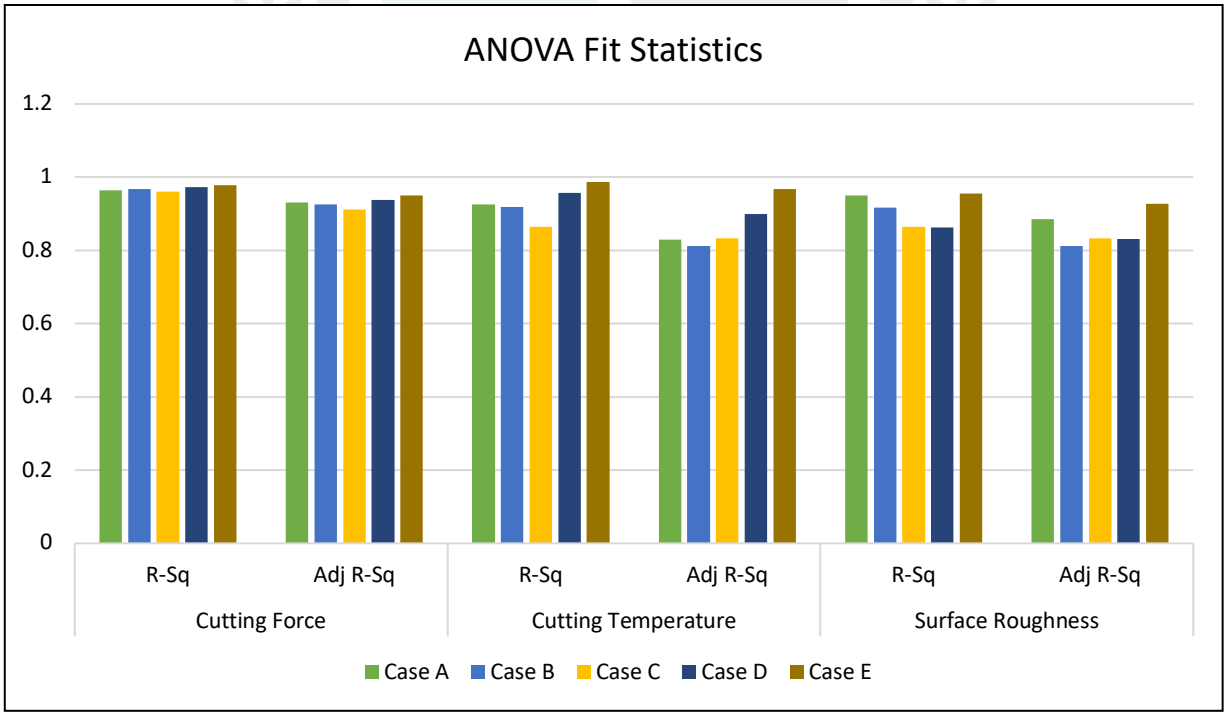

Fig. 2 ANOVA Fit Statistics for comparisons of all cooling strategies

Analysis of Variance (ANOVA) was performed to evaluate the statistical significance of the developed models for cutting force, cutting temperature, and surface roughness across the different cooling strategies (Cases A, B, C, D and E). The ANOVA results confirmed that the quadratic models for each machining response were highly significant, with "Lack-of-Fit" values appearing non-significant, thereby validating the adequacy of the models. The coefficient of determination (R sq) and adjusted coefficient of determination (Adj. sq), which represent the proportion of variance captured by the models, are presented in the Fit Statistics in Fig. 2.

As illustrated in the fit statistics of Fig. 2, Case E cooling strategy exhibits superior correlation coefficients compared to remaining all across all measured machining responses. The R sq and Adjusted R sq values for Case E reached 0.9781 and 0.9499 for cutting force, 0.9859 and 0.9677 for cutting temperature, and 0.9549 and 0.9278 for surface roughness, respectively. Given that higher values of R sq and Adjusted R sq signify a

more robust and reliable model fit, Case E was selected as the most suitable candidate for further detailed analysis and optimization.

STATISTICAL ANALYSIS OF OUTPUT PARAMETERS FOR CASE E

In this experimental investigation, the cutting force and cutting temperature were monitored in real-time during the turning operation, while the surface roughness was characterized post-machining. Statistical analysis was performed using Design-Expert 13 software (maintaining a 95% confidence interval) to evaluate the output responses and generate diagnostic plots, including perturbation and 3D surface plots.

The following sections provide a detailed discussion of the statistical analysis regarding the influence of process factors on the machining characteristics. For Case E (Al_2O_3:ZnO at a 75:25 ratio), the ANOVA results derived from the regression analysis and the predictive models generated by the software are presented below:

A. CUTTING FORCE

The ANOVA results for cutting force (Table 10) confirm the significance of the developed quadratic model ($p<0.05$). The feed rate was found to be the most significant parameter ($p<0.0001$), followed by nanoparticle concentration ($p=0.0004$) and cutting speed ($p=0.0178$).

The quadratic effect of the nanoparticle concentration (2 wt%) also showed a very low p-value (0.0001), indicating its substantial influence on the overall force response. Based on these p-values, the quadratic model provides a robust and accurate representation of the cutting force variations in the hybrid Al_2O_3-ZnO environment.

Table 10. ANOVA results for cutting force

Source	Sum of Squares	Mean Square	F-value	p-value	
Model	76942.88	8549.21	34.68	< 0.0001	significant
A-Cutting Speed	2339.06	2339.06	9.49	0.0178	
B-Wt% of NP	9845.39	9845.39	39.94	0.0004	
C-Feed	45210.54	45210.54	183.41	< 0.0001	
AB	0.6947	0.6947	0.0028	0.9591	
AC	1802.85	1802.85	7.31	0.0304	
BC	2605.11	2605.11	10.57	0.0140	
A^2	193.88	193.88	0.7865	0.4046	
B^2	14944.60	14944.60	60.63	0.0001	
C^2	314.96	314.96	1.28	0.2956	
Residual	1725.51	246.50			
Lack of Fit	1428.91	476.30	6.42	0.0521	not significant
Pure Error	296.60	74.15			
Cor Total	78668.40				

Fig. 3 illustrates the perturbation effects of the process parameters at the center points: cutting speed (69.63 m/min), nanoparticle concentration (1 wt%), and feed rate (0.18 mm/rev). An increase in the feed rate leads to a corresponding rise in cutting force due to the larger volume of the uncut chip. Conversely, the cutting force is observed to decrease with an increase in cutting speed, likely due to thermal softening at the shear zone. Regarding the hybrid nanofluid, the cutting force is higher at the extremes (0 and 2 wt%) but reaches a minimum at 1 wt%. This phenomenon is attributed to the high thermal conductivity of Al_2O_3 nanoparticles, which facilitates rapid heat dissipation from the tool-workpiece interface. Simultaneously, the ZnO nanoparticles

provide high colloidal stability, allowing for the formation of a persistent lubricating film that reduces friction and lowers the overall turning force.

Fig. 4 presents the 3D response surface plot illustrating the interaction between nanoparticle concentration and cutting speed at a constant feed rate of 0.18 mm/rev. The surface topography reveals that the minimum cutting force is achieved at a cutting speed of 69.63 m/min with a 1 wt% nanoparticle concentration. Conversely, the highest cutting force is observed at the lowest cutting speed (31.71 m/min) under dry MQL conditions (0 wt%). This "valley" in the response surface at 1 wt% confirms that the hybrid Al_2O_3-ZnO particles significantly reduce the mechanical load compared to base-oil MQL, particularly as the cutting speed increases and facilitates better lubricant penetration.

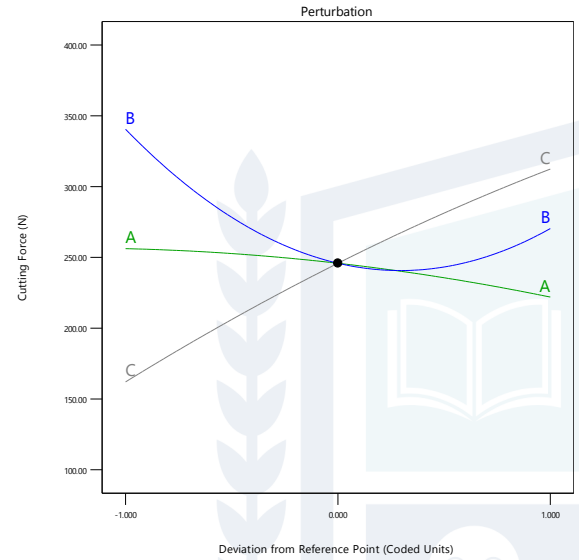

Fig. 3 Cutting force perturbation plot

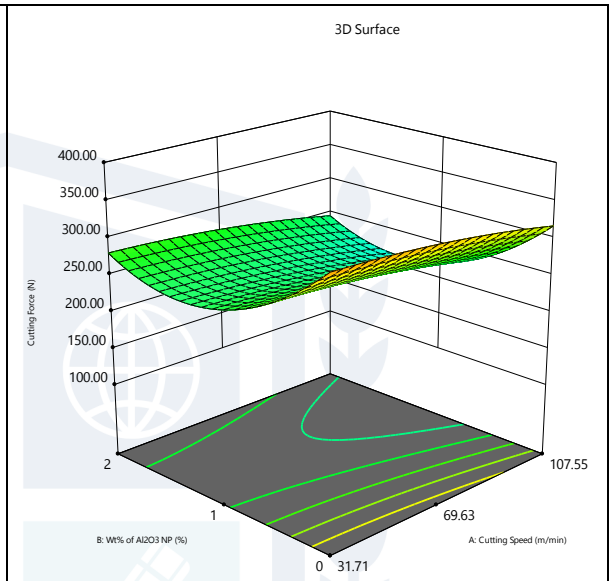

Fig. 4 3D surface plot for cutting force

B. CUTTING TEMPERATURE

The statistical modeling of the cutting temperature follows a quadratic trend, which is verified as statistically significant ($p<0.05$). The ANOVA breakdown in Table 11 reveals that cutting speed and nanoparticle loading (both linear and quadratic terms) exert a primary influence on the temperature ($p<0.0001$). However, the lack of significant interaction effects indicates that the combined impact of speed and concentration does not deviate from their individual trends.

Table 11. ANOVA results for cutting temperature

Source	Sum of Squares	Mean Square	F-value	p-value	
Model	3282.38	364.71	54.21	< 0.0001	Significant
A-Cutting Speed	468.33	468.33	69.62	< 0.0001	
B-Wt% of NP	1390.23	1390.23	206.66	< 0.0001	
C-Feed	190.22	190.22	28.28	0.0011	
AB	100.90	100.90	15.00	0.0061	
AC	0.8100	0.8100	0.1204	0.7388	
BC	3.71	3.71	0.5508	0.4821	
A^2	18.82	18.82	2.80	0.1384	
B^2	1121.24	1121.24	166.67	< 0.0001	
C^2	4.68	4.68	0.6953	0.4319	

Residual	47.09	6.73			
Lack of Fit	29.47	9.82	2.23	0.2271	not significant
Pure Error	17.62	4.41			
Cor Total	3329.47				

Fig. 5 displays the impact of input parameters on cutting temperature. As expected, increases in cutting speed and feed rate result in higher temperatures due to increased friction and plastic deformation. The temperature is significantly reduced at a 1 wt% nanoparticle concentration compared to 0 wt.%, followed by a slight rebound at 2 wt%. The primary cooling mechanism is the enhanced heat transfer capability provided by the Al_2O_3 nanoparticles, which possess high thermal conductivity. This allows the hybrid nanofluid to remove heat from the tool-workpiece interface more rapidly than conventional MQL, though the benefit stabilizes after the 1 wt% mark.

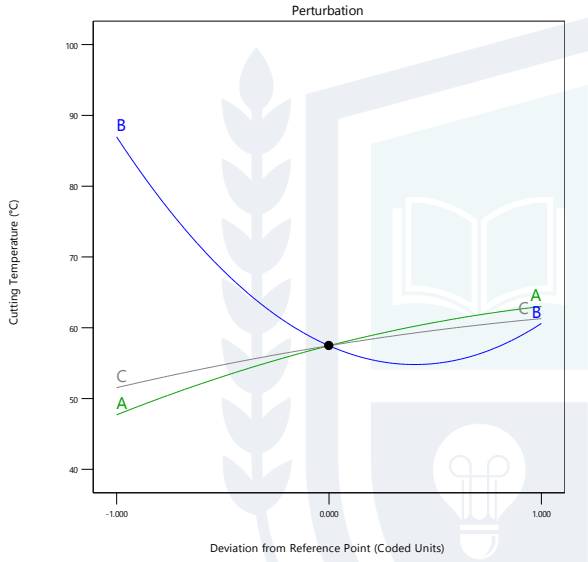

Fig. 5 Cutting temperature perturbation plot

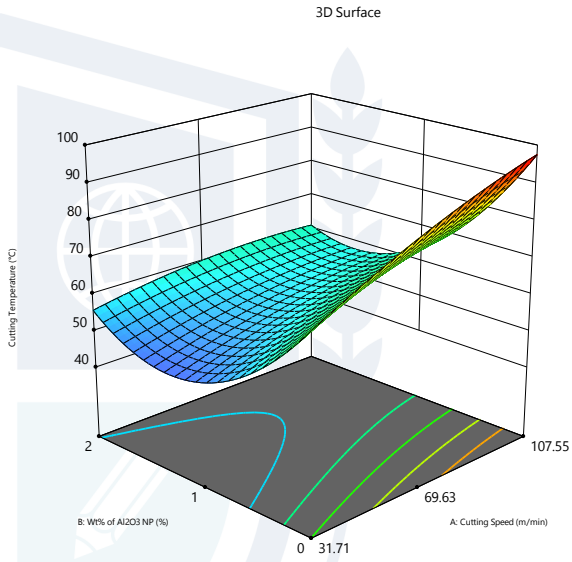

Fig. 6 3D surface plot for cutting temperature

Fig. 6 shows the 3D response surface for cutting temperature. The results highlight that the minimum temperature is achieved at 69.63 m/min and 1 wt% NP concentration. Conversely, the maximum cutting temperature is reached at 31.71 m/min with 0 wt% NP. This visual representation underscores the superior cooling capacity of the 1 wt% hybrid nanofluid, which significantly lowers the interface temperature compared to the base-oil MQL across the investigated speed range.

C. SURFACE ROUGHNESS

The final output response evaluated in this study is the surface roughness of the machined specimens. The regression analysis yielded a statistically significant quadratic model ($p<0.05$), confirming its adequacy for predicting surface quality. According to the ANOVA results in Table 12, the feed rate and nanoparticle concentration (wt%) were identified as the most dominant factors, while the interaction terms between the variables were found to be non-significant. This suggests that the influence of the hybrid nanofluid on surface topography remains consistent across different feed regimes.

Table 12. ANOVA results for surface roughness

Source	Sum of Squares	Mean Square	F-value	p-value	
Model	4.36	0.7261	35.27	< 0.0001	significant
A-Cutting Speed	0.2578	0.2578	12.52	0.0054	

B-Wt% of NP	0.7206	0.7206	35.01	0.0001	
C-Feed	3.00	3.00	145.51	< 0.0001	
AB	0.1132	0.1132	5.50	0.0410	
AC	0.2688	0.2688	13.06	0.0047	
BC	0.0008	0.0008	0.0381	0.8492	
Residual	0.2058	0.0206			
Lack of Fit	0.1735	0.0289	3.58	0.1187	not significant
Pure Error	0.0323	0.0081			
Cor Total	4.56				

Fig. 7 illustrates the perturbation effects of the process parameters on surface roughness at the center levels: cutting speed (69.63 m/min), nanoparticle concentration (1 wt%), and feed rate (0.18 mm/rev). The analysis reveals a positive correlation between all three input factors and surface roughness. While the feed rate is the primary driver of roughness due to the increased height of the feed marks, the rise in cutting speed also contributes to surface degradation, likely through elevated tool-tip vibrations.

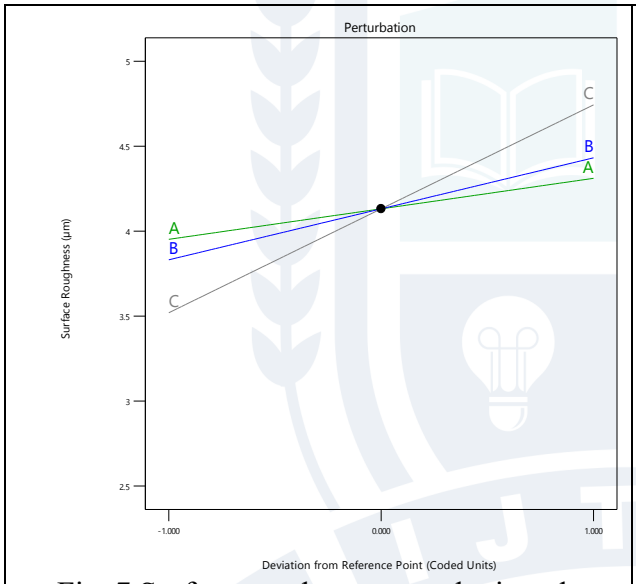

Fig. 7 Surface roughness perturbation plot

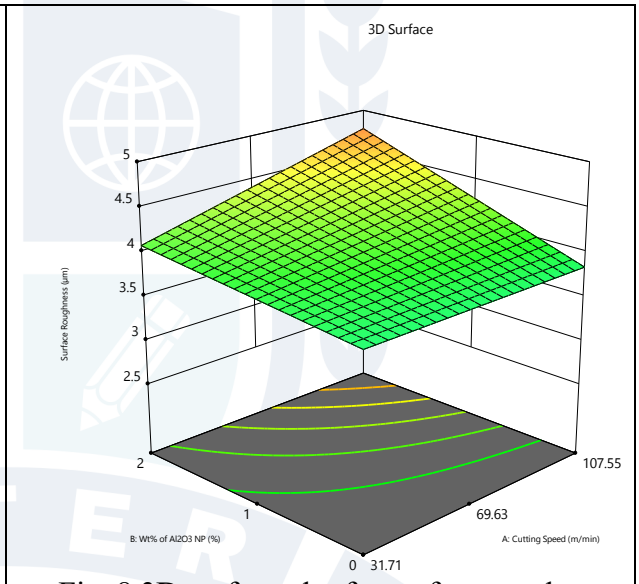

Fig. 8 3D surface plot for surface roughness

Furthermore, the 3D response surface plot in Fig. 8 shows that the minimum surface roughness is achieved at the lowest cutting speed (31.71 m/min) and 0 wt% concentration. Conversely, the maximum roughness occurs at the highest speed (107.55 m/min) and 2 wt% loading, suggesting that excessive nanoparticle concentrations may hinder the effective atomization of the MQL mist, thereby negatively impacting the surface integrity.

V. Discussion

The experimental results demonstrate that a hybrid nanoparticle proportion of 75:25 (Al_2O_3:ZnO) consistently achieved the most favorable outcomes for cutting force, cutting temperature, and surface roughness. This configuration outperformed both alternative hybrid ratios and the base-oil MQL (0 wt%). The enhancement in performance is primarily attributed to the increased thermal conductivity of the nanofluid when nanoparticles are added up to a moderate level (1 wt%). This improved thermal profile, combined with the synergistic lubricating effects of the hybrid particles, is the fundamental driver behind the significant reduction in machining responses during the turning operation.

The quadratic RSM-Box-Behnken models developed for cutting force, cutting temperature, and surface roughness demonstrated high adequacy, evidenced by strong coefficients of determination (R^2) and non-significant lack-of-fit values. This confirms the models' reliability in capturing the complex influences of

machining parameters and nanofluid composition. A clear functional distinction emerged between the two systems: Al_2O_3 consistently yielded superior surface finish, particularly at low-to-moderate feed rates. Furthermore, the spherical morphology of nanoparticles, as reported by [35] is attributed to the formation of a protective tribo-film and the "micro-bearing" action of the Alumina particles, which significantly enhances tribological performance and reduces friction [4]. Conversely, ZnO exerted a stronger influence on cutting temperature due to its superior thermal conductivity, which facilitates efficient heat dissipation at elevated cutting speeds [39].

VI. Optimization with Validation

Following the statistical characterization of the process parameters, the next objective was to identify the optimal machining conditions. This study employs the Box-Behnken RSM to determine the ideal levels for both input and output variables. Upon identifying these optimal settings, a validation experiment was conducted to verify the predictive accuracy of the RSM models. The primary goal of this confirmatory trial was to validate the conclusions drawn from the statistical analysis and to quantify the actual improvement in machining performance achieved at the optimized parameter levels.

Optimization of the turning process was conducted by setting specific goals for both input and output parameters. The input parameters (Speed, wt.% NP, and Feed) were constrained to their experimental ranges, while the output responses (Force, Temperature, and Roughness) were targeted for minimization. Table 13. Constraint criteria table for optimum conditionoutlines these constraint criteria, which were utilized by the Design-Expert software to determine the optimal levels for high-performance hybrid nano-MQL machining.

Table 13. Constraint criteria table for optimum condition

Parameter	Goal	Lower Limit	Upper Limit	Lower Weight	Upper Weight
A:Cutting Speed	is in range	31.71	107.55	1	1
B:Wt% of NP	is in range	0	2	1	1
C:Feed	is in range	0.11	0.25	1	1
Cutting Force	minimize	148.757	392.24	1	1
Cutting Temperature	minimize	43.21	97.84	1	1
Surface Roughness	minimize	2.996	4.979	1	1

Multi-objective optimization was performed to identify the best machining configuration, yielding an exceptionally high desirability value of 0.985. The optimal settings were determined to be a cutting speed of 31.71 m/min, a nanoparticle concentration of 1 wt%, and a feed rate of 0.11 mm/rev. To ensure the statistical integrity of these results, a series of confirmatory experiments was initiated. This involved conducting three independent experimental runs at the predicted optimal levels to verify the consistency and reproducibility of the output responses (cutting force, temperature, and surface roughness).

Table 14. Validation experimentation run for optimum parameters confirmation

Output Parameter	Optimum input level	Predicted value by RSM	Experiment value
Cutting Force	Cutting Speed: 31.71 m/min, Wt% of NP: 1 and Feed: 0.11 mm/rev	148.76	146.57
Cutting Temperature	Cutting Speed: 31.71 m/min, Wt% of NP: 1 and Feed: 0.11 mm/rev	41.0537	42.1
Surface Roughness	Cutting Speed: 31.71 m/min, Wt% of NP: 1 and Feed: 0.11 mm/rev	3.08594	3.082

Table 14 presents a comparative analysis between the software-predicted values and the actual experimental results obtained at the optimized parameter levels The data reveals a high degree of correlation, with the measured output parameters showing a "good agreement" with the predicted intervals. This close proximity between the theoretical and experimental values confirms the statistical validity of the developed RSM models and ensures that the identified control parameters effectively optimize the machining performance.

VII. CONCLUSION

The present study demonstrates that both mono and hybrid nanofluids under MQL can improve the turning performance of AISI 1040 steel within the investigated parameter ranges. The RSM–Box–Behnken regression models show good agreement with experimental results, confirming their adequacy for predicting cutting temperature, cutting force, and surface roughness. Among all cases, Case E (75:25 Al_2O_3:ZnO hybrid nanofluid) gave the best overall machining performance. The hybrid fluid improved heat transfer and lubrication, while the mono nanofluids showed more limited benefits, with Al_2O_3 performing better for cutting force and surface roughness and ZnO performing better for temperature control. Cutting force, cutting temperature, and surface roughness generally increased with higher cutting speed, feed, and nanoparticle concentration. The optimum condition for Case E was 31.71 m/min cutting speed, 0.11 mm/rev feed, and 1 wt% nanoparticles, which gave the highest desirability and close agreement between predicted and measured results. Overall, the study shows that hybrid nanofluid-based MQL is a promising approach for sustainable turning of AISI 1040 steel.

The scope of this experimental study is limited to the selected range of cutting parameters and the specific material–tool combination employed. Important aspects such as tool life, residual stress distribution, and the long-term stability of the Al_2O_3–ZnO mixture were not examined. In addition, the study does not include a detailed assessment of the economic or environmental implications of nanoparticle usage. These issues offer valuable directions for future research to further develop the optimized hybrid nanofluid MQL framework established in this work.

VIII. REFERENCES

[1] A. M. Khan *et al.*, "Multi-objective optimization for grinding of AISI D2 steel with Al2O3 wheel under MQL," *Materials*, vol. 11, no. 11, 2018, doi: 10.3390/ma11112269.

[2] K. V. Ramanan, S. Ramesh Babu, M. Jebaraj, and K. Nimel Sworna Ross, "Face turning of Incoloy 800 under MQL and nano-MQL environments," *Materials and Manufacturing Processes*, vol. 36, no. 15, pp. 1769–1780, 2021, doi: 10.1080/10426914.2021.1944191.

[3] V. S. Sharma, G. Singh, and K. Sorby, "A review on minimum quantity lubrication for machining processes," *Materials and Manufacturing Processes*, vol. 30, no. 8, pp. 935–953, Aug. 2015, doi: 10.1080/10426914.2014.994759.

[4] A. K. Sharma, A. K. Tiwari, and A. R. Dixit, "Effects of Minimum Quantity Lubrication (MQL) in machining processes using conventional and nanofluid based cutting fluids: A comprehensive review," Jul. 20, 2016, *Elsevier Ltd*. doi: 10.1016/j.jclepro.2016.03.146.

[5] Y. K. Hwang and C. M. Lee, "Surface roughness and cutting force prediction in MQL and wet turning process of AISI 1045 using design of experiments," *Journal of Mechanical Science and Technology*, vol. 24, no. 8, pp. 1669–1677, 2010, doi: 10.1007/s12206-010-0522-1.

[6] T. Leppert, "Effect of cooling and lubrication conditions on surface topography and turning process of C45 steel," *Int. J. Mach. Tools Manuf.*, vol. 51, no. 2, pp. 120–126, 2011, doi: 10.1016/j.ijmachtools.2010.11.001.

[7] C. H. Che Haron, J. A. Ghani, M. S. Kasim, T. K. Soon, A. I. Gusri, and M. A. Sulaiman, "Surface integrity of Inconel 718 under MQL condition," in *Advanced Materials Research*, 2011, pp. 1667–1672. doi: 10.4028/www.scientific.net/AMR.150-151.1667.

[8] M. Hadad and B. Sadeghi, "Minimum quantity lubrication-MQL turning of AISI 4140 steel alloy," *J. Clean. Prod.*, vol. 54, pp. 332–343, 2013, doi: 10.1016/j.jclepro.2013.05.011.

[9] Z. Liu, Q. An, J. Xu, M. Chen, and S. Han, "Wear performance of (nc-AlTiN)/(a-Si3N4) coating and (nc-AlCrN)/(a-Si3N4) coating in high-speed machining of titanium alloys under dry and minimum quantity lubrication (MQL) conditions," *Wear*, vol. 305, no. 1–2, pp. 249–259, Jul. 2013, doi: 10.1016/j.wear.2013.02.001.

[10] A. Saini, S. Dhiman, R. Sharma, and S. Setia, "Experimental estimation and optimization of process parameters under minimum quantity lubrication and dry turning of AISI-4340 with different carbide inserts," *Journal of Mechanical Science and Technology*, vol. 28, no. 6, pp. 2307–2318, 2014, doi: 10.1007/s12206-014-0521-8.

[11] S. M. Agrawal and N. G. Patil, "Experimental study of non edible vegetable oil as a cutting fluid in machining of M2 Steel using MQL," in *Procedia Manufacturing*, Elsevier B.V., 2018, pp. 207–212. doi: 10.1016/j.promfg.2018.02.030.

[12] P. Sivaiah, M. Guru Prasad, M. Singh M, and B. Uma, "Machinability evaluation during machining of AISI 52100 steel with textured tools under Minimum Quantity Lubrication–A comparative study," *Materials and Manufacturing Processes*, vol. 35, no. 15, pp. 1761–1768, Nov. 2020, doi: 10.1080/10426914.2020.1802034.

[13] G. Singh, V. Aggarwal, and S. Singh, "Experimental investigations into machining performance of Hastelloy C-276 in different cooling environments," *Materials and Manufacturing Processes*, vol. 36, no. 15, pp. 1789–1799, 2021, doi: 10.1080/10426914.2021.1945099.

[14] P. Sivaiah, V. Ajay kumar G, K. Lakshmi Narasimhamu, and N. Siva Balaji, "Performance improvement of turning operation during processing of AISI 304 with novel textured tools under minimum quantity lubrication using hybrid optimization technique," *Materials and Manufacturing Processes*, 2021, doi: 10.1080/10426914.2021.1967977.

[15] N. Chavda and R. Bumataria, "Effect of Particle Size and Concentration on Thermal Performance of Cylindrical Shaped Heat Pipe Using Silver-DI Water Nanofluid," *International Journal of Ambient Energy*, pp. 1–20, 2022, doi: https://doi.org/10.1080/01430750.2022.2127887.

[16] R. Bumataria and N. Chavda, "Heat load and orientation impacts in cylindrical heat pipes using copper oxide, aluminium oxide, and zinc oxide nanofluids," *International Journal of Ambient Energy*, 2021, doi: 10.1080/01430750.2021.2014957.

[17] R. K. Bumataria, N. K. Chavda, and H. Panchal, "Current research aspects in mono and hybrid nanofluid based heat pipe technologies," *Heliyon*, vol. 5, no. 5, p. e01627, 2019, doi: 10.1016/j.heliyon.2019.e01627.

[18] R. K. Bumataria, N. K. Chavda, and A. H. Nalbandh, "Performance evaluation of the cylindrical shaped heat pipe utilizing water-based CuO and ZnO hybrid nanofluids," *Energy Sources, Part A: Recovery, Utilization and Environmental Effects*, vol. 00, no. 00, pp. 1–16, 2020, doi: 10.1080/15567036.2020.1832628.

[19] R. Padmini, P. Vamsi Krishna, and G. Krishna Mohana Rao, "Effectiveness of vegetable oil based nanofluids as potential cutting fluids in turning AISI 1040 steel," *Tribol. Int.*, vol. 94, pp. 490–501, Feb. 2016, doi: 10.1016/j.triboint.2015.10.006.

[20] S. N. Rao, B. Satyanarayana, and K. Venkatasubbaiah, "Experimental estimation of tool wear and cutting temperatures in MQL using cutting fluids with CNT inclusion," *International Journal of Engineering Science and Technology*, vol. 3, no. 4, pp. 2928–2931, Apr. 2011.

[21] M. Amrita, R. R. Srikant, A. V. Sitaramaraju, M. M. S. Prasad, and P. V. Krishna, "Experimental investigations on influence of mist cooling using nanofluids on machining parameters in turning AISI 1040 steel," *Proceedings of the Institution of Mechanical Engineers, Part J: Journal of Engineering Tribology*, vol. 227, no. 12, pp. 1334–1346, Dec. 2013, doi: 10.1177/1350650113491934.

[22] M. Amrita, S. A. Shariq, M. Manoj, and C. Gopal, "Experimental investigation on application of emulsifier oil based nano cutting fluids in metal cutting process," *Procedia Eng.*, vol. 97, pp. 115–124, 2014, doi: 10.1016/j.proeng.2014.12.231.

[23] A. K. Sharma, A. K. Tiwari, R. K. Singh, and A. R. Dixit, "Tribological Investigation of TiO2 Nanoparticle based Cutting Fluid in Machining under Minimum Quantity Lubrication (MQL)," *Mater. Today Proc.*, vol. 3, no. 6, pp. 2155–2162, 2016, doi: 10.1016/j.matpr.2016.04.121.

[24] P. Rapeti, V. K. Pasam, K. M. Rao Gurram, and R. S. Revuru, "Performance evaluation of vegetable oil based nano cutting fluids in machining using grey relational analysis-A step towards sustainable manufacturing," *J. Clean. Prod.*, vol. 172, pp. 2862–2875, Aug. 2016, doi: 10.1016/j.jclepro.2017.11.127.

[25] V. K. Pasam, R. R. Srikant, and S. Gugulothu, "Comparing the performance & viability of nano and microfluids in minimum quantity lubrication for machining AISI1040 steel," in *Materials Today: Proceedings*, Elsevier Ltd, 2018, pp. 8016–8024. doi: 10.1016/j.matpr.2017.11.486.

[26] R. Padmini, V. P. Krishna, S. Mahith, and S. Kumar, "Influence of Green Nanocutting Fluids on Machining Performance Using Minimum Quantity Lubrication Technique," 2019. doi: https://doi.org/10.1016/j.matpr.2019.06.612.

[27] A. K. Sharma, R. K. Singh, A. R. Dixit, and A. K. Tiwari, "Novel uses of alumina-MoS2 hybrid nanoparticle enriched cutting fluid in hard turning of AISI 304 steel," *J. Manuf. Process.*, vol. 30, pp. 467–482, Dec. 2017, doi: 10.1016/j.jmapro.2017.10.016.

[28] R. K. Singh, A. K. Sharma, A. R. Dixit, A. K. Tiwari, A. Pramanik, and A. Mandal, "Performance evaluation of alumina-graphene hybrid nano-cutting fluid in hard turning," *J. Clean. Prod.*, vol. 162, pp. 830–845, Sep. 2017, doi: 10.1016/j.jclepro.2017.06.104.

[29] M. Jamil *et al.*, "Effects of hybrid Al2O3-CNT nanofluids and cryogenic cooling on machining of Ti–6Al–4V," *International Journal of Advanced Manufacturing Technology*, vol. 102, no. 9–12, pp. 3895–3909, 2019, doi: 10.1007/s00170-019-03485-9.

[30] Ç. V. Yıldırım, "Experimental comparison of the performance of nanofluids, cryogenic and hybrid cooling in turning of Inconel 625," *Tribol. Int.*, vol. 137, pp. 366–378, Sep. 2019, doi: 10.1016/j.triboint.2019.05.014.

[31] A. Thakur, A. Manna, and S. Samir, "Experimental investigation of nanofluids in minimum quantity lubrication during turning of EN-24 steel," *Proceedings of the Institution of Mechanical Engineers, Part J: Journal of Engineering Tribology*, vol. 234, no. 5, pp. 712–729, May 2019, doi: 10.1177/1350650119878286.

[32] P. B. Zaman, M. I. H. Tusar, and N. R. Dhar, "Selection of appropriate process inputs for turning Ti-6Al-4V alloy under hybrid Al2O3-MWCNT nano-fluid based MQL," *Advances in Materials and Processing Technologies*, 2020, doi: 10.1080/2374068X.2020.1812324.

[33] M. Sandeep Kumar, V. Vasu, and A. Venu Gopal, "Investigation of Influence of Hybrid Nanofluid/MQL on Surface Roughness in Turning Inconel-718," *Advances in Applied Mechanical Engineeering*, pp. 1137–1145, 2020, doi: http://doi.org./10.1007/978-981-15-1201-8_120.

[34] M. Sandeep Kumar, V. Murali Krishna, and M. Kumar, "Investigation on influence of Hybrid Biodegradable Nanofluids (CuO-ZnO) on Surface Roughness in Turning AISI 1018 Steel," 2020. doi: 10.1016/j.matpr.2020.04.477.

[35] S. Haghnazari and V. Abedini, "Effects of hybrid Al2O3–CuO nanofluids on surface roughness and machining forces during turning AISI 4340," *SN Appl. Sci.*, vol. 3, no. 2, Feb. 2021, doi: 10.1007/s42452-020-04088-w.

[36] K. Apmann, R. Fulmer, A. Soto, and S. Vafaei, "Thermal Conductivity and Viscosity: Review and Optimization of Effects of Nanoparticles," *Materials*, vol. 14, no. 5, p. 1291, Mar. 2021, doi: 10.3390/ma14051291.

[37] T. M. Duc, T. B. Ngoc, N. M. Tuan, and T. T. Long, "An optimization study on Al2O3 nanoparticle concentration, air pressure, and air flow rate in MQL hard turning," *Advances in Mechanical Engineering*, vol. 17, no. 9, Sep. 2025, doi: 10.1177/16878132251381542.

[38] F. Günan, T. Kıvak, Ç. V. Yıldırım, and M. Sarıkaya, "Performance evaluation of MQL with AL2O3 mixed nanofluids prepared at different concentrations in milling of Hastelloy C276 alloy," *Journal of Materials Research and Technology*, vol. 9, no. 5, pp. 10386–10400, Sep. 2020, doi: 10.1016/j.jmrt.2020.07.018.

[39] M. B. Naim Shaikh, A. Rosenkranz, M. Ali, and S. A. Ahmad, "Improving the performance of cutting fluids by using ZnO and ZrO2 nanoparticles," *Proceedings of the Institution of Mechanical Engineers, Part N: Journal of Nanomaterials, Nanoengineering and Nanosystems*, Jul. 2024, doi: 10.1177/23977914241263453.

Abbreviations	
Al_2O_3	Aluminium Oxide
ANOVA	Analysis of Variance
ZnO	Zinc Oxide
NP	Nanoparticle
NF	Nanofluid
DOE	Design of Experimentation
RSM	Response Surface Methodology
wt%	Weight Fraction (%)
v%	Volume Fraction (%)